METER-SCALE TOPOGRAPHIC ROUGHNESS OF ASTEROID (101955) BENNU FROM THE OSIRIS-REX LASER ALTIMETER. F. M. Rossmann[1], C. L. Johnson[1,2], E. B. Bierhaus[3], O. S. Barnouin[4], Department of Earth, Ocean and Atmospheric Sciences, University of British Columbia, Vancouver, Canada, [2]Planetary Science Institute, Tucson, AZ, USA, [3]Lockheed Martin Space, Littleton, CO, USA, [4]Johns Hopkins University Applied Physics Laboratory, Laurel, MD, USA.

Introduction: Images and lidar measurements of the surface of asteroid (101955) Bennu from the OSIRIS-REx Camera Suite (OCAMS) [1] and the OSIRIS-REx Laser Altimeter (OLA) [2] have revealed evidence for different geologic resurfacing processes acting over a range of spatial scales. Boulders can be broken down by micro-meteorite bombardment, fracturing induced by thermal stresses, and space-weathering, all of which act on short timescales to produce finer-grained materials [3]. OCAMS images reveal that the geographical distribution of boulders and regolith on Bennu is heterogeneous, with evidence for mass movement of material toward the equatorial bulge, particle self-organization, and particle-size grading along the flow direction [4]. Impact cratering can modify the surface by fragmentation of the target material, excavation of the subsurface, and production of an ejecta field. Observations indicate that the particle size-frequency distribution of granular material excavated in impact craters varies across craters of different sizes [5]. The efficiency of formation of small craters on Bennu is governed by an impact-armouring effect, evidenced in the crater record by a paucity of craters with diameters < 2.5 m [6].

Here, we analyze surface roughness, calculated from OLA data, to further investigate spatial variations in boulders and fine-grained material across Bennu. We focus on roughness interior and exterior to craters, and on global variations in the scale-length dependence of roughness.

Data and Methods: We used OLA Science Level 2A (L2A) v21 point clouds from the Orbital B phase of the mission [7], produced by the OSIRIS-REx Altimetry Working Group. These point clouds have been globally registered to minimize differences among overlapping, individual OLA scans. The OLA spot size during the Orbital B global mapping phase was ~7.5 cm diameter [7].

We use two metrics to estimate roughness: (1) the RMS height roughness metric, $\xi(L)$ of [8], and (2) the RMS deviation, $\nu(L)$, or the root of the mean-square differences in height of points separated by a lag or baseline distance [8]. We calculate both roughness metrics for baseline lengths, L, from 0.5 – 25 m.

We first combined and down-sampled the L2A data to a 5 cm point cloud to produce a data set with a more uniform spatial data density that was also more manageable in size. We then established nodes spaced

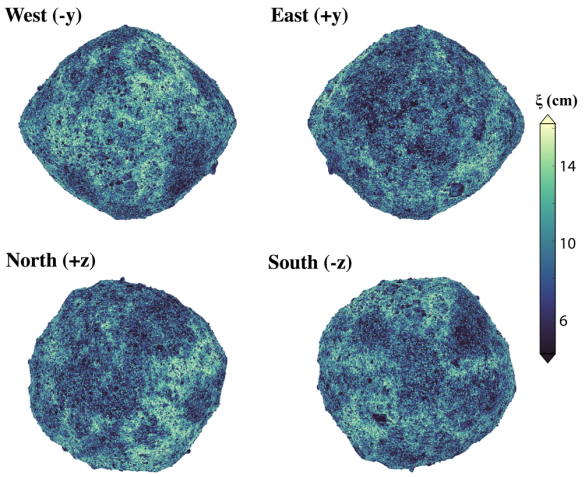

Figure 1: Global point-clouds for the detrended RMS height roughness metric, ξ, for a baseline length of 2.5 m. Bright regions are associated with high abundances of boulders at length scales near the baseline length. The spatial distribution of roughness is heterogeneous and large-scale structure related to large impact structures is visible.

~ 25 cm apart. For each node, a kd-tree neighbour-in-radius search was implemented on the 5 cm point cloud. Neighbors within a specified radius r (corresponding to a baseline length, L, where $r = L/2$ for $\xi(L)$, and $r = L$ for $\nu(L)$) of the node were binned and detrended with a best-fitting plane estimated using orthogonal distance regression. The mean position of the binned points and the variability (standard deviation) of orthogonal heights above the regression plane were calculated, yielding ξ. This algorithm can be easily modified to calculate $\nu(L)$ of [8] by finding the difference in orthogonal heights between the node and neighbouring points that are separated by a lag distance of L, and then computing $\nu(L)$ locally using these height differences. $\xi(L)$ and $\nu(L)$ were calculated for 8 baseline lengths between 0.5 and 25 m ($B \in [0.5, 25]$ m). We used the results for ξ or ν to fit median roughness versus baseline length with a power-law. The power-law exponent, H (the Hurst or Hausdorff exponent), describes the self-affinity of roughness with length scale for the underlying surface, and has been computed for other planetary bodies, e.g. in [9, 10].

Results and Discussion: Figure 1 shows a global OLA point cloud of Bennu colored by $\xi(L)$ calculated for L = 2.5 m. In general, we find a spatial correlation of surface roughness with boulder density when the

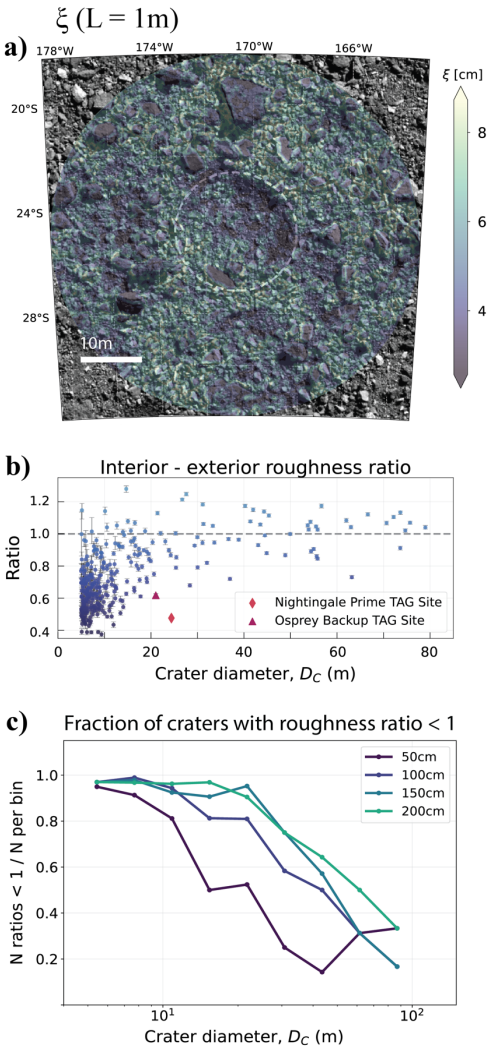

Figure 2: (a) OCAMS image mosaic of a 20 m diameter impact crater (dashed white line) superposed with roughness (color scale) at the 1 m baseline. (b) Interior-exterior roughness ratio for 345 craters versus crater diameter for the 1 m baseline. (c) Binned fraction of craters with roughness ratio significantly less than 1 versus crater diameter for 0.5, 1, 1.5, and 2 m baselines.

average dimension of boulders is smaller than L. Boulders with average major axis lengths smaller than, but approaching L, typically appear 'rougher' than boulders with dimensions << L, as the latter have a smaller topographic expression. An example of this is seen in Figure 2a, which shows $\xi(L = 1\text{ m})$ for a 20 m diameter impact crater. Regions with the lowest roughness (dark blue) are associated with finer grained material mostly inside the crater, and with the smooth, flat faces of large boulders outside the crater. Bright regions indicate a higher abundance of particles with axis lengths close to 1 m, that are mostly exterior to the crater.

Craters: We analyzed the roughness, $\xi(L)$ interior and exterior to craters for a global population of 345 craters with diameters 5 – 80 m using the RMS height surface roughness and for baseline lengths L = 0.5, 1, 1.5 and 2 m. For each crater and choice of L we computed the ratio of interior/exterior surface roughness for each crater (e.g. Figure 2b for L = 1 m). We also calculated the fraction of craters in a given diameter range that have an interior/exterior roughness ratio significantly less than 1. We find that a substantial population of craters, especially those with small diameters have lower interior roughness than their surroundings (Figure 2b) and that this relationship is baseline dependent (Figure 2c). This supports other work that suggests the presence of a finer-grained sub-surface layer on Bennu, evidenced in crater morphologies [5].

Hurst exponent: Using baselines from 0.5 m to 25 m, we create roughness maps with 0.25 degree resolution and estimate the Hurst exponent, H, for each pixel. This yields a global map of H which condenses the roughness information from individual roughness maps for each baseline length. We find a median global Hurst exponent of 0.66 +/- 0.07 using the RMS deviation, and 0.71 +/- 0.07 using the RMS height, where the ranges indicate the 25th and 75th percentiles. Preliminary results show that regions enhanced in small particles and having a low abundance of large boulders have a comparatively lower Hurst exponent compared to regions dominated by large boulders. This result is consistent with the idea that visually 'smooth' or finer-grained regions have smoother topography at large scales relative to small scales. Regions with the largest estimated values for H are associated with Bennu's largest boulders and with large-scale impact structures bordered by high concentrations of large boulders.

Acknowledgments: This work was enabled by the collaborative efforts of the OSIRIS-REx Team, supported by NASA under Contract NNM10AA11C issued through the New Frontiers Program. The OLA instrument build and Canadian science support were provided by contracts with the Canadian Space Agency.

References: [1] Rizk, B. et al. (2018). *SSR*, v. 214, 26. [2] Daly, M. G., et al. (2017). *SSR*, v. 212, 899–924. [3] DellaGiustina D. N. et al (2020) *Science,* 370. [4] Jawin, E. R. et al. (2022), *Icarus,* 381, 114992. [5] Bierhaus E. B. et al. (2020), *LPSC MMXX,* Abstract #2156. [6] Bierhaus, E. B. et al., (2022), *Nat. Geosci.*, 15, 440-446. [7] Seabrook, J. A. et al, (2022), *Planet. Sci. J.*, 3 265. [8] Shepherd, M. K et al. (2001), *JGR., 106*, 32,777–32,795. [9] Rosenburg, M. A. et al, (2011), *JGR*, 11, EO2001. [10] Susorney, H. C. M. et al, (2019), *Icarus*, 325, 141-152.